

Time-saving method for directly amplifying and capturing
a minimal amount of pancreatic tumor-derived mutations
from fine-needle aspirates using digital PCR

(微量組織検体中の体細胞変異の検出を可能にする
迅速デジタルPCR解析法の開発)

旭川医科大学医学部
旭川医科大学大学院医学系研究科博士課程
臨床消化器学領域 専攻
林 明宏

(Ono Y, Maeda C, Suzuki M, Wada R, Sato H, Kawabata H, Okada T, Goto T,
Karasaki H, Mizukami Y, Okumura T)

Supplementary Information

Time-saving method for directly amplifying and capturing a minimal amount of pancreatic tumor-derived mutations from fine-needle aspirates using digital PCR

Yusuke Ono, Akihiro Hayashi, Chiho Maeda, Mayumi Suzuki, Reona Wada, Hiroki Sato, Hidemasa Kawabata, Tetsuhiro Okada, Takuma Goto, Hidenori Karasaki, Yusuke Mizukami, and Toshikatsu Okumura

This PDF file includes:

SI Materials and Methods

Fig. S1 and S2

Table S1 and S2

SI Materials and Methods

Targeted amplicon sequencing

A pancreatic ductal carcinomas (PDA)-associated gene panel (Ion AmpliSeq Custom DNA Panel) was designed using the Ion AmpliSeq Designer 3.6, to analyze the coding DNA sequences +25 bp away from the intronic flanking regions for 8 genes, namely *KRAS*, *TP53*, *SMAD4*, *CDKN2A*, *GNAS*, *PIK3CA*, *BRAF*, and *STK11*. The customized panel consisted of 42 amplicons in a single primer pool with a total of 4.7 kb DNA that covered 100% of the regions of interest, as shown in the BED file obtained from the Ion AmpliSeq Cancer Hotspot Panel v2 (Thermo Fischer Scientific) (Supplementary Table). DNA (10–60 ng) was amplified using this panel, and a sequencing library was prepared. Sequencing and data analyses were performed using the Ion S5 GeneStudio system (Thermo Fisher Scientific, Waltham, MA, USA) as described previously [1]. Sequenced reads were demultiplexed, quality-filtered, and aligned to the human reference genome (GRCh37), using the Torrent Suite software package (ver. 5.0.4; Thermo Fisher Scientific). The mapping module (Torrent Mapping Alignment Program) is a sequence alignment software program optimized specifically for Ion Torrent data and includes several mapping algorithms with specific applications. Mapping was performed using default parameter values. Variants were identified using the Variant Caller plugin (ver. 5.0.4.0; Thermo Fisher Scientific) and included in the Torrent Suite Package, which was optimized to exploit the underlying flow signals. Variant calling analysis was performed using the somatic variant calling mode, which was optimized to detect low-frequency variants. The set parameters were as follows: minimum allele frequency, 0.02; minimum coverage, 100. To identify somatic mutations, the independent genotyping results for tumor and normal samples were excluded, and

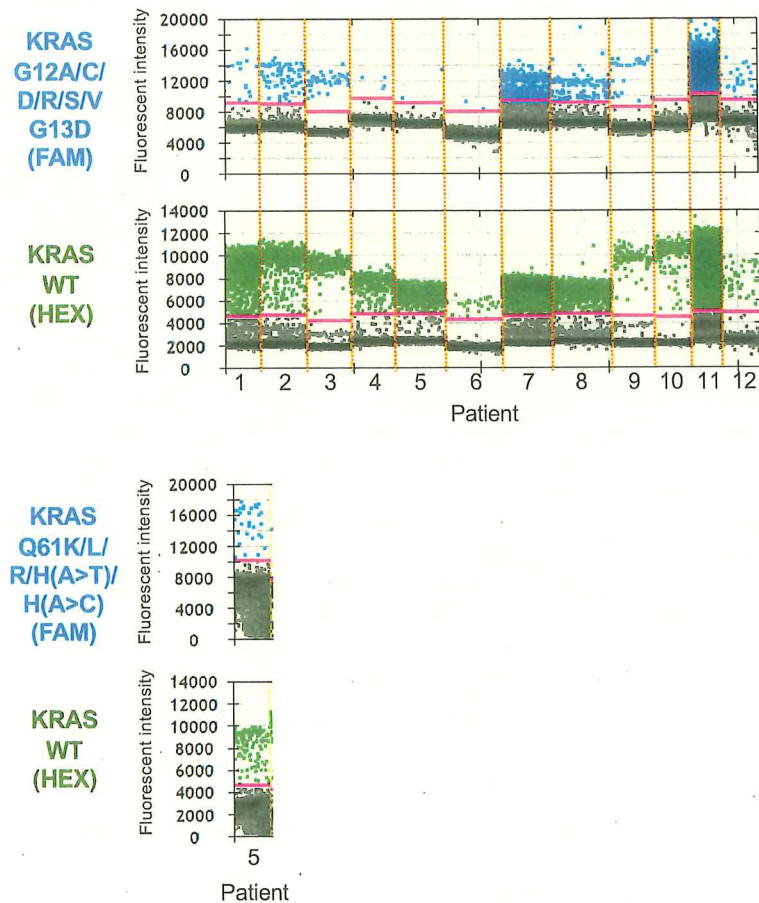
variants in the normal samples were excluded from the molecular profile. Putative false-negative variants were excluded by analyzing the Phred-scale quality score, which was calculated using this plugin and manually confirming the alignment with IGV software (version 2.3.59; <http://software.broadinstitute.org/software/igv/>).

For variants containing novel exonic, nonsynonymous, and frameshift variants as well as intronic splice variants, the COSMIC (<http://cancer.sanger.ac.uk/cosmic>) and ClinVar databases (<https://www.ncbi.nlm.nih.gov/clinvar/>) were used for classification as either pathogenic or a variants with an unknown significance [2].

SI References

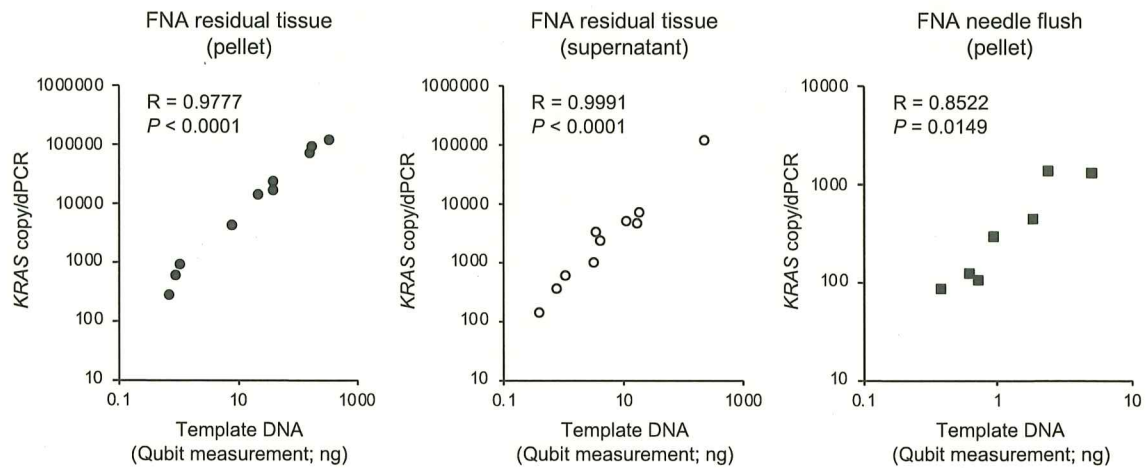
- 1 Nagai, K. et al. Metachronous intraductal papillary mucinous neoplasms disseminate via the pancreatic duct following resection. *Mod Pathol* (2019).
- 2 Omori, Y. et al. Pathways of progression from intraductal papillary mucinous neoplasm to pancreatic ductal adenocarcinoma based on molecular features. *Gastroenterology* **156**, 647-661 e642 (2019).

Supplementary Figure 1: dPCR results for the resected pancreata



Twenty microliters of the resuspension was mixed with 10 μ L of ddPCR Supermix for Probes (Bio-Rad) and 1 μ L of ddPCR *KRAS* Screening Multiplex Kit (targets for G12A/C/D/R/S/V and G13D), and vortexed. After the reaction mixture was encapsulated in droplets using the QX200 droplet generator (Bio-Rad), PCR was performed; the endpoint fluorescence intensity of each droplet was counted and the copy number was calculated using QuantaSoft (ver 1.7; Bio-Rad), which was based on the Poisson distribution. The threshold line (solid pink line) was manually set to extend 2,000 or 1,000 amplitude (FAM mutant probe or HEX wild-type probe) above the maximum value for the background intensity. Table 1 shows the numerical data for dPCR and clinical profiles for each patient.

Supplementary Figure 2: Correlation between amplifiable DNA indexed by the copy number of *KRAS* and the amount of template DNA



Correlation between amplifiable DNA indexed by the copy number of *KRAS* from FNA samples and the amount of template DNA quantified using a Qubit fluorometer. Pearson's correlation coefficients and *P*-values are shown for FNA residual tissue and needle flush (see Supplementary Table 2 for more details).

Supplementary Table 1: Covered region of NGS panel used in this study

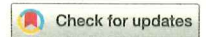
Amplicon No.	Chromosome	Start	End	Gene
1	chr3	178916775	178916881	PIK3CA
2	chr3	178916931	178917035	PIK3CA
3	chr3	178921464	178921570	PIK3CA
4	chr3	178927405	178927525	PIK3CA
5	chr3	178927901	178927986	PIK3CA
6	chr3	178928069	178928160	PIK3CA
7	chr3	178936023	178936105	PIK3CA
8	chr3	178938787	178938918	PIK3CA
9	chr3	178947818	178947896	PIK3CA
10	chr3	178951996	178952097	PIK3CA
11	chr3	178952140	178952237	PIK3CA
12	chr7	140453102	140453221	BRAF
13	chr7	140481391	140481515	BRAF
14	chr9	21970940	21971066	CDKN2A
15	chr9	21971090	21971219	CDKN2A
16	chr12	25378549	25378658	KRAS
17	chr12	25380260	25380364	KRAS
18	chr12	25398186	25398304	KRAS
19	chr17	7573923	7574035	TP53
20	chr17	7577015	7577151	TP53
21	chr17	7577508	7577612	TP53
22	chr17	7578180	7578298	TP53
23	chr17	7578352	7578483	TP53
24	chr17	7578516	7578601	TP53
25	chr17	7579350	7579485	TP53
26	chr17	7579853	7579960	TP53
27	chr18	48575099	48575213	SMAD4
28	chr18	48575556	48575677	SMAD4
29	chr18	48581190	48581302	SMAD4
30	chr18	48584551	48584678	SMAD4
31	chr18	48586251	48586361	SMAD4
32	chr18	48591814	48591931	SMAD4
33	chr18	48593399	48593519	SMAD4
34	chr18	48603028	48603119	SMAD4
35	chr18	48604658	48604774	SMAD4
36	chr19	1206977	1207104	STK11
37	chr19	1220310	1220450	STK11
38	chr19	1220480	1220603	STK11
39	chr19	1221236	1221332	STK11
40	chr19	1223014	1223144	STK11
41	chr20	57484396	57484504	GNAS
42	chr20	57484562	57484672	GNAS

Sequencing DNA panels, which were custom designed to target the 8 PDA-related genes (*KRAS*, *TP53*, *SMAD4*, *CDKN2A*, *GNAS*, *PIK3CA*, *BRAF*, and *STK11*), consisted of 42 amplicons, with a total of 4.7 kb of DNA.

Supplementary Table 2: Copy number of KRAS amplified using qPCR assay and concentration of purified DNA from FNA residual tissues end needle flush


Patient	FNA residual tissue													
	Pellet				Supernatant				FNA needle flush					
	Water-burst		Purified DNA		Water-burst		Supernatant		Water-burst		Supernatant			
wild-type KRAS (copies/reaction)	mutant KRAS (copies/reaction)	Amount of template DNA (ng)	wild-type KRAS (copies/reaction)	mutant KRAS (copies/reaction)	wild-type KRAS (copies/reaction)	mutant KRAS (copies/reaction)	Amount of template DNA (ng)	wild-type KRAS (copies/reaction)	mutant KRAS (copies/reaction)	wild-type KRAS (copies/reaction)	mutant KRAS (copies/reaction)	Amount of template DNA (ng)	wild-type KRAS (copies/reaction)	mutant KRAS (copies/reaction)
1	292	94	43.6	12,900	2,720	no call	no call	12.06	2,740	2,060	64	5.382	762	466
2	no call	no call	182	45,000	20,200	no call	no call	234	77,800	28,700	no call	2,502	850	460
3	164	130	376.8	76,200	32,600	no call	no call	19.35	4,420	2,260	38	0.765	86	15
4	260	66	23.4	7,820	5,420	no call	no call	1.143	350	176	24	N/A	280	112
5	112	15.2	1.161	3,080	966	no call	no call	3.636	2,120	888	42	N/A	130	20
6	770	159.2	8.631	538	316	no call	no call	0.774	220	110	11.4	0.657	60	54
7	3366	10.92	43.6	21,560	no call	no call	no call	3.276	884	no call	no call	N/A	24	no call
8	78.6	12.4	0.756	208	40	no call	no call	4.086	1,480	572	12	N/A	222	50
9	230	no call	0.952	548.6	no call	no call	no call	0.424	126	no call	440	0.408	80	no call
	(302)	(36.8)		(366.6)	(78)	(no call)	(no call)		(130)	(11)	(42)		(92)	(5.8)
10	8900	4460	188	47,040	34,650	no call	no call	16.92	2,680	1,434	158	1.9	270	158

Note: no call; Neither KRAS mutant nor wild-type allele was detected by digital PCR. Parentheses indicate results of KRAS Q61 mutation assay (patient 9) Abbreviations; N/A, data not available



OPEN

Time-saving method for directly amplifying and capturing a minimal amount of pancreatic tumor-derived mutations from fine-needle aspirates using digital PCR


Yusuke Ono^{1,2,3}, Akihiro Hayashi^{2,3}, Chiho Maeda¹, Mayumi Suzuki¹, Reona Wada¹, Hiroki Sato², Hidemasa Kawabata², Tetsuhiro Okada², Takuma Goto², Hidenori Karasaki¹, Yusuke Mizukami^{1,2}  & Toshikatsu Okumura²

It is challenging to secure a cytopathologic diagnosis using minute amounts of tumor fluids and tissue fragments. Hence, we developed a rapid, accurate, low-cost method for detecting tumor cell-derived DNA from limited amounts of specimens and samples with a low tumor cellularity, to detect *KRAS* mutations in pancreatic ductal carcinomas (PDA) using digital PCR (dPCR). The core invention is based on the suspension of tumor samples in pure water, which causes an osmotic burst; the crude suspension could be directly subjected to emulsion PCR in the platform. We examined the feasibility of this process using needle aspirates from surgically resected pancreatic tumor specimens ($n = 12$). We successfully amplified and detected mutant *KRAS* in 11 of 12 tumor samples harboring the mutation; the positive mutation frequency was as low as 0.8%. We used residual specimens from fine-needle aspiration/biopsy and needle flush processes ($n = 10$) for method validation. In 9 of 10 oncogenic *KRAS* pancreatic tumor samples, the "water-burst" method resulted in a positive mutation call. We describe a dPCR-based, super-sensitive screening protocol for determining *KRAS* mutation availability using tiny needle aspirates from PDAs processed using simple steps. This method might enable pathologists to secure a more accurate, minimally invasive diagnosis using minute tissue fragments.

Abbreviations

dPCR Digital PCR
FNA Fine-needle aspiration
PDA Pancreatic ductal adenocarcinoma

It is challenging to acquire histological evidence regarding solid tumors non-invasively; this hamper clinical management decisions that need to be made at appropriate time points. Fine-needle aspiration (FNA) is a standard procedure for collecting tumor tissues; however, there are cases where inadequate sampling resulted in false negative results¹. This technical issue might be highlighted when tumors, including pancreatic ductal adenocarcinomas (PDAs), which have a low tumor cell content, are targeted. Because of the invasiveness of needle-assisted cytology and biopsy as well as the potential for tumor cell dissemination, albeit at a low incidence, the frequent repetition of the procedure is not generally recommended^{2,3}.

¹Institute of Biomedical Research, Sapporo Higashi Tokushukai Hospital, Sapporo, Hokkaido 065-0033, Japan. ²Division of Gastroenterology and Hepatology/Oncology, Department of Medicine, Asahikawa Medical University, Asahikawa, Hokkaido 078-8510, Japan. ³These authors contributed equally: Yusuke Ono and Akihiro Hayashi. email: mizu@asahikawa-med.ac.jp

The assessment of the tumor grade and histological type is an essential task for pathologists; however, there are possibilities of inter-pathologist diagnostic disagreement⁴. Information regarding the expression levels of specific tumorigenesis-associated proteins in routine clinical practice enables pathologists to reach a consensus on the matter⁵. Limited amounts of specimens can also be an obstacle for performing additional molecular analysis, which emphasizes the necessity of alternative tools that provide evidence regarding malignant tumors⁶.

A robust solution might involve the detection of frequently mutated genes in a specific type of cancer⁷. For instance, in human PDAs, the *KRAS* gene is ubiquitously mutated, and in over 90–95% of patients, lesions emerged because of oncogenic events at the earliest periods of the tumorigenesis process⁸. Another initiating driver mutation in *KRAS* has been reported in colorectal (40%) and lung adenocarcinomas (15–20%). Mutations in other types of tumors, including *BRAF* mutations in melanomas (50–90%) and papillary thyroid carcinomas (50%), *EGFR* mutations in lung cancer, and *PIK3CA* mutations in colorectal and breast cancer might be used as genetic markers for the early identification of malignant tumors^{9–12}.

Recent technological advances in genetics such as sequencing and PCR-based genetic analysis might allow the super-sensitive and absolute quantification of very low levels of mutant alleles, even in a small yield of tumor samples with shallow cellular content¹³. Here, we sought to further develop a new digital PCR (dPCR) protocol using tissues collected from pancreatic tumors by FNA, which allows for the detection of genetic mutations in small amounts of specimens. In pre-clinical settings, by obtaining tumor specimens right after resection, a high accuracy of detection of tumor cell-derived DNA via dPCR was achieved. By eliminating the genomic DNA purification process, the sample could be processed in a simple and rapid manner and subsequent analysis could be conducted; this may support the routine clinical diagnosis.

Results

Development of a method to detect the minimal copy number of tumor-derived mutant *KRAS*. We investigated a method for detecting mutations in tiny tissue samples using absolute quantification via dPCR. To prepare input DNA from the samples, we first tested two methods, to avoid losses during the nuclear purification step. In the first method, cells/tissues were encapsulated using the droplet generator, and the PCR reaction was then directly performed. We performed serial dilution using two different cell lines, i.e. MIA PaCa-2 (homozygous *KRAS* G12C) and NB1RGB (wild-type *KRAS*). The ratios of mutants to wild-type genes in cell mixtures were 20:4,000, 100:4,000, 500:4,000, and 1,000:4,000. The cells suspended in 4 μ L of PBS were directly enclosed within emulsion drops (Fig. 1A), using the QX200 system, and then used for the dPCR mutation detection assay. As shown in Fig. 1C, the frequency of detection of mutations after the capture of the enclosed cells was modest (12.9% in *KRAS* mutant cells or 2.9% in wild-type *KRAS* cells, on average).

We, therefore, examined the alternative method, where cells were collected and resuspended in nuclease-free water, which caused an osmotic burst of collected cells; this could cause genomic DNA to be released into the liquid fraction (Fig. 1B). The “crude” DNA was then directly utilized as the dPCR template without performing the DNA purification step (around 30 min); hence, throughout the assay, we could determine the *KRAS* mutation status in fresh tumor samples within 2.5 h (a few minutes of preparation of tumor-derived DNA before processing dPCR). The dPCR reaction proceeded successfully even with impure DNA, and the detection of the *KRAS* copy number was comparable to that for the sample prepared through conventional DNA purification (Fig. 1C). These results suggested that the “water-burst” method could be used to perform both timesaving preparation steps and achieve high-efficiency detection of small numbers of DNA copies.

Mutation detection analysis using fresh needle-aspirated tissues from resected pancreatic neoplasia. Next, we examined the feasibility of detecting *KRAS* mutants using a tiny amount of resected tumor tissue. Twelve patients with pancreatic tumors were enrolled, and the needle aspirates from the tumor and the non-tumor areas of the resected specimens were analyzed. The aspirates were suspended in nucleus-free water following storage and spin-down. In the dPCR assay, *KRAS* G12/G13 mutations were found in the PDA from 10 patients, including IPMN-associated pancreatic cancers; 1 PDA patient exhibited mutant *KRAS* Q61H. In contrast, no *KRAS* mutation was detected in tumors in a patient with a pancreatic neuroendocrine tumor (Table 1). Multiple *KRAS* mutations were found in the tumor obtained from one patient with IPMN-associated carcinoma.

Using the “water-burst” method, we successfully detected the *KRAS* G12/G13 mutations in the fresh needle aspirates from 10 PDAs with corresponding mutations. Besides, the *KRAS* Q61 mutation was found in 1 sample from a patient exhibiting *KRAS* Q61H mutation, while the number of *KRAS* G12/G13 mutations was below the cut-off value (Table 1, Supplementary Figure). We found a 100% concordance in *KRAS* mutations in a small tumor cohort including a sample with wild-type *KRAS*. The lowest frequency in the mutation to wild-type in these patients was 0.82% (mutation allele frequency in the primary tumor lesion was 12.8%; Table 1).

Detection of *KRAS* mutations via dPCR using residual tissues of endoscopic biopsy samples. We attempted to validate the capture of dPCR-based driver mutations via the “water-burst” method using a residual piece of tumor tissue in the FNA needle. After submitting pancreatic tumor biopsy specimens to the pathology laboratory, minimal amounts of the remaining samples were collected to test the “water-burst” method, by scratching the residual tissues from Petri dishes and flushing the needle with the stabilizing solution (Fig. 2A). The fluid was preserved, shipped, and centrifuged before genetic analysis. Then, the pellets suspended in water and the supernatants were analyzed via the dPCR assay, which targeted *KRAS* mutations. In 9 of 10 patients, we found *KRAS* mutations in residual tissues (G12/G13 mutants in 8 patients, Q61 mutant in 1 patient) obtained after FNA. In 7 specimens of needle-rinsed fluids, we detected G12/G13 mutations in 6 patients, and Q61 mutation in 1 patient (Table 2, Fig. 2B). In patient 7, who was diagnosed with a pancreatic acinar cell car-

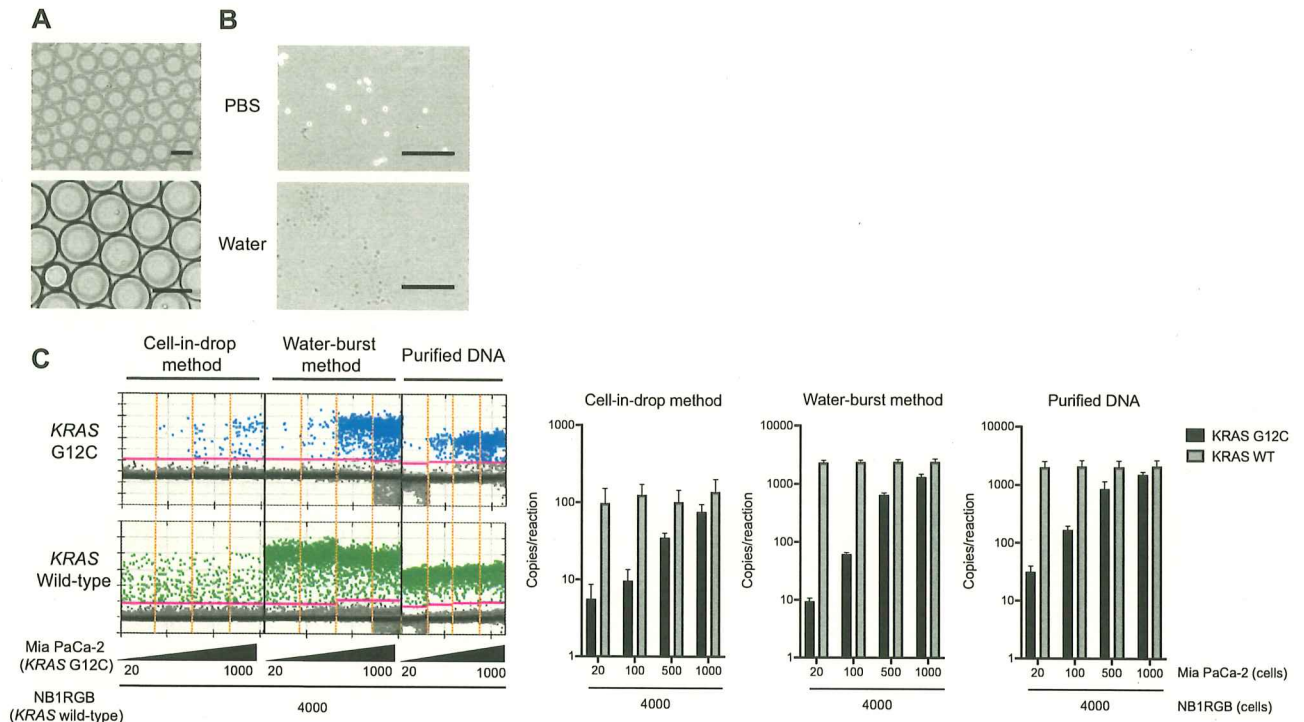


Figure 1. Experimental results using cell lines to improve the dPCR method for the highly sensitive mutation analysis of simple prepared samples. (A) Encapsulated cells in dPCR droplets. Cells were collected, resuspended in dPCR reaction solution, and mixed with droplet generation oil using the QX200 droplet generator. Scale bars; 200 μm . (B) Cells were burst using pure water. Cells were collected and resuspended in nuclease-free water, which caused an osmotic burst of cells, and genomic DNA was released into the water. The “crude” solution, including gDNA, was used as the dPCR template. Scale bars; 500 μm . (C) The dPCR assay was performed using the two novel DNA preparation methods, without a purification step. *KRAS* wild-type (Fibroblast; NB1RGB) and *KRAS* G12C (PDA; MIA PaCa-2) cells were mixed with several dilution series (left panel). The wild-type or G12C mutation in *KRAS* was detected using the QX200 droplet reader, as compared to the conventional DNA preparation method using commercial purification kits (see details in “Methods”). The *KRAS* copy number of wild-type or G12C measured by QuantaSoft software (right panel).

cinoma exhibiting no *KRAS* mutations, the level of the *KRAS* G12/G13 variant was found to be approximately similar to the detection limit of the screening kit (0.2%). In contrast, the mutation allele frequency in other samples with mutant *KRAS* was over 10%. Either the residual tissue or needle flush part of the FNA samples was also analyzed using dPCR assay following DNA purification (Table 2). A strong correlation was observed between amplified *KRAS* copy numbers and the amount of template DNA (Supplementary Table 2 and Supplementary Fig. 2). The “water-burst” assay using pellets from FNA residual tissue showed a *KRAS* mutant allele frequency equivalent to that of purified DNA except for patient 2, whereas the supernatants required DNA purification.

To confirm the fact that the *KRAS* mutations identified using this method originated from the tumor, pathological specimens from FFPE blocks were genotyped via targeted amplicon sequencing. In all 9 samples in which mutant *KRAS* was detected by the “water-burst” method, the *KRAS* mutation was pathologically proven to be present in the PDA tissue. In one patient with a *KRAS* G12D tumor, we failed to detect mutations during the FNA-needle flush process, while we could identify the mutation using DNA that was purified and concentrated from the supernatant and water-bursting of the residual tissue in FNA-needles (Table 2; patient 8). Another patient with an absent mutation calling in *KRAS*, as observed by the “water-burst” dPCR assay, was pathologically diagnosed as having a pancreatic acinar cell carcinoma with no *KRAS* mutations (patient 7). Taken together, the mutation detection method, and rapid and easy sample preparation rendered it highly feasible for us to identify *KRAS* mutations in small amounts of tissues.

Discussion

The genetic profiling of solid tumors enables us to understand the molecular signatures of tumor development and progression more effectively; it also provides clinically relevant information for an early diagnosis, and pharmacological vulnerability and resistance towards various types of cancer⁸. The safer acquisition of cancer cells or tissue sampling sometimes makes it difficult for pathologists to secure a proper diagnosis. Recently, genetic tests utilizing a biopsy specimen have been more commonly used for patients with lung and colorectal cancer, for the selection of chemotherapeutic reagents; this generally requires a certain amount of tissues with a high tumor-cell content^{14,15}. However, there are cases where a low tumor cellularity, as well as a tiny amount of tumor specimens per se hampered molecular analysis^{16,17}. Besides, although DNA extraction/purification has been

Patient	Age	Sex	Surgically resected specimens				Fresh tissue aspirates			
			Pathological diagnosis	Histological type	Tumor cellularity*	Mutation profiles of KRAS (%MAF on targeted sequencing)	Wild-type KRAS (copy/reaction)	G12/G13 mutant KRAS (copy/reaction)	KRAS G12/G13 MAF (%)	Results of KRAS G12/G13 screening in the dPCR assay**
1	68	F	PDA	Mod	Mod	G12V (12.8)	2,130	18	0.82	Positive
2	76	M	Acinar cell carcinoma	N/A	High	G12D (16.6)	640	112	15.97	Positive
3	69	F	IPMN-associated PDA	Mod	Mod	G12D (18.8)	538	68	10.84	Positive
4	77	M	IPMN-associated PDA	Well	Low	G12D (6.6)	5,100	100	1.92	Positive
5	54	F	PDA	Por	Low	Q61H (31.5)	11,980	10	0.09	Negative (Q61mutation 13.6%***)
6	76	M	IPMN	Low-grade	Mod	G12D (24.7), G12V (21.4), G12S (1.0)	400	22	5.21	Positive
7	81	F	PDA	Mod	Mod	G12V (5.0)	105,580	9,383	8.16	Positive
8	69	M	PDA	Por	Mod	G12D (43.8)	15,500	1,220	7.30	Positive
9	65	M	IPMN	High-grade	Mod	G12V (39.9)	5,053	2,413	32.32	Positive
10	61	F	P-NET	G-1	High	WT	2,025	4	0.20	Negative
11	71	M	IPMN-associated PDA	Por	Mod	G12D (7.4)	17,560	14,910	45.92	Positive
12	70	M	IPMN	High-grade	Mod	G12V (18.6)	90	78	46.43	Positive

Table 1. KRAS mutation analysis in punctured specimens obtained from resected pancreatic tumor tissues. IPMN intraductal papillary mucinous neoplasm, MAF mutant allele frequency, PDA pancreatic ductal adenocarcinoma, P-NET pancreatic neuroendocrine tumor. *Tumor cellularity; low, <10%, medium, 10–30%, high, >30%. **Mutation detection assay was performed using ddPCR KRAS G12/G13 Screening Multiplex Kit (Bio-Rad); cut-off >0.2%. ***For the case with KRAS Q61 positive lesion determined by target sequencing, additional dPCR was performed by ddPCR KRAS Q61 Screening Kit (Bio-Rad); cut-off >0.5%.

routinely performed for genetic testing, the process is time- and cost-consuming and sometimes significantly dilutes the target molecule. Here, we used specimens from patients with pancreatic cancer, which is characterized by a very low tumor cell content and abundant desmoplasia; these are challenging biospecimens not only for conventional immunohistochemistry analysis, but also for molecular analysis.

In this study, we evaluated a DNA preparation method without the purification step, for the genetic testing of the FNA specimen obtained from the pancreas, using the dPCR platform. We tried two different methods; the “cell-in-droplet” method involved the direct enclosure of the target cells into the droplet, followed by dPCR, while the “water-burst” approach attempted to capture tumor-derived DNA, following the osmotic burst of cancer cells, by their exposure to pure water just before their compartmentalization during the dPCR. We found that the latter approach was superior to the “cell-in-droplet” method. In the “water-burst” method, we could detect even a small number of cells with a homozygous KRAS mutation at codon 12, in as low as 20 cells (=40 copies) in 4,000 normal cells with wild-type KRAS, showing that it was feasible to detect dPCR-based direct driver mutations in crude tumor tissues. We found this method to be clinically relevant, as it demonstrated that the KRAS mutation was detected in needle aspirates, with the tumor lesion cells being detected in 11 of 12 needle aspirates obtained from surgically resected pancreatic tissues, and in 9 of 10 residual tumor cells obtained from FNA needles, after sending the core specimens to the pathology lab. These results indicated that the combination of the “water-burst” approach and dPCR technology has the potential for detecting mutations in a super-sensitive manner, in a specimen with low-tumor cell content, such as a pancreatic tumor.

FNA is the gold standard for pathological diagnosis in patients with different types of cancer, including PDA, owing to its high diagnostic accuracy¹⁸. Because of tumor heterogeneity, multiple punctures might be required to avoid failure during pathological assessment. Occasionally, the report was based on the assessment of a limited number of cancer cells, and the use of insufficient amounts of tumor tissues for sampling can result in false-negative results. On the other hand, the dilemma associated with FNA involves the potential risk of bleeding and needle tract seeding at the puncture site^{3,19}. The detection of genetic mutations might compensate for limitations in pathological assessment, and the utility of such a strategy has been demonstrated^{13,20}.

Next-generation sequencing (NGS)-based gene panel testing has been an invaluable tool in cancer diagnostics^{7,21}. This modality offers a great deal of information related to genetic variation from a single sample, and over time, it has become much easier to operate. Nevertheless, a certain amount of high-quality DNA from an abundant of tumor tissue requiring multiple FNA punctures is required. Besides, the handling duration for the sample preparation, library quantification, and sequencing was long²². The limit of detection of mutations is >1%, unless additional library preparation processes, such as molecular barcoding are employed, which would make the assay more expensive and time-consuming. Besides, careful bioinformatics assessments, such as those

for error elimination and reporting are required to translate the data to the clinic²³. On the other hand, the dPCR assay requires only a small amount of sample (1–5 ng of DNA), and the frequency of detected mutations is as low as 0.05%²⁴. The running cost for dPCR is affordable, and it serves as an excellent filter for identifying high-risk patients.

The most distinctive feature of this study was that we could save on the effort, cost, and time required for DNA purification by simply suspending the stored material in water and breaking the cells. Molecular tests involving dPCR have not been used widely in the clinic²⁵. This new method would potentially play an active, significant role in routine examinations. Because of the ease of sample preparation, operations with a high mobility during testing caused the confinement of regions of genes in a small number of samples, such as that observed during the compensatory assessment using the dPCR-method for the cytopathology test. The only parameter to ensure sample quality in the water-burst method is currently the copy number of *KRAS* amplified. A strong correlation was observed between the copy number and the amount of template DNA when the purification step was included in the same sample sets. Additional parameters such as DNA fragment size may help to precisely determine the quality of the crude samples.

We used a commercially validated screening probe set for detecting multiple *KRAS* codon 12/13 mutations using a small amount of tissue sample. There are several limitations associated with using this probe set. The first is that in this study, false positives (0.27% in FNA residual tissues) were observed. The threshold of the mutation frequency determined by the assay manufacturer was 0.2%. In the crude DNA used in this method, impurities existed or DNA was fragmented, because the degrading enzymes secreted from cells might have resulted in non-specific signals for mutations. In the future, it would become necessary to determine the cut-off value unique to our method, by using a larger number of tumor specimens in clinical settings.

The second issue was that screening probe set we utilized could detect multiple *KRAS* mutations at codons 12, 13, or 61; this does not provide accurate information associated with specific variations in mutations. Pancreatic neoplasia has often evolved with various distributed clonal backgrounds^{8,26}; therefore, it is essential to determine each mutation pattern, to accurately identify primary lesions or the existence of coexisting malignant or benign lesions. Besides, a mutation in *KRAS* alone is not sufficient to provide genetic evidence of pancreatic cancer. Therefore, improvement of the current protocol targeting related mutations in other driver genes and tumor suppressors, such as *TP53* and *SMAD4*, is warranted. To solve this problem, we are currently developing a novel multiplex analysis method that identifies major *KRAS* and other gene mutations using 2D-spatial information regarding fluorescence intensity in dPCR. The dPCR system we used can distinguish two fluorescent colors²⁷; however, a novel dPCR platform would be capable of simultaneously detecting multi-color dyes. Such a new tool might further enhance the utility of the assay during multiplex analysis, potentially allowing the detection of driver mutations across multiple genomic regions²⁸.

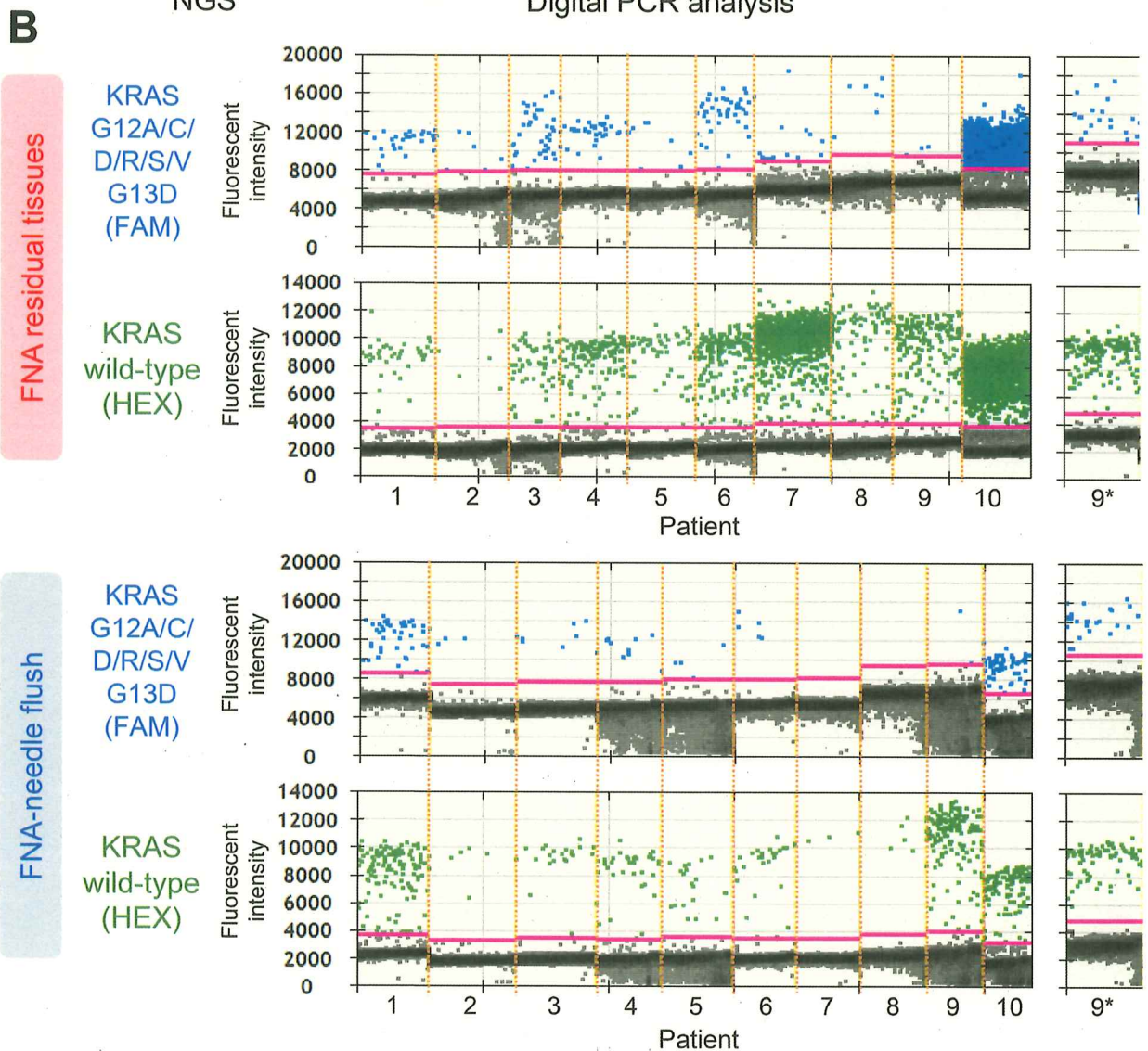
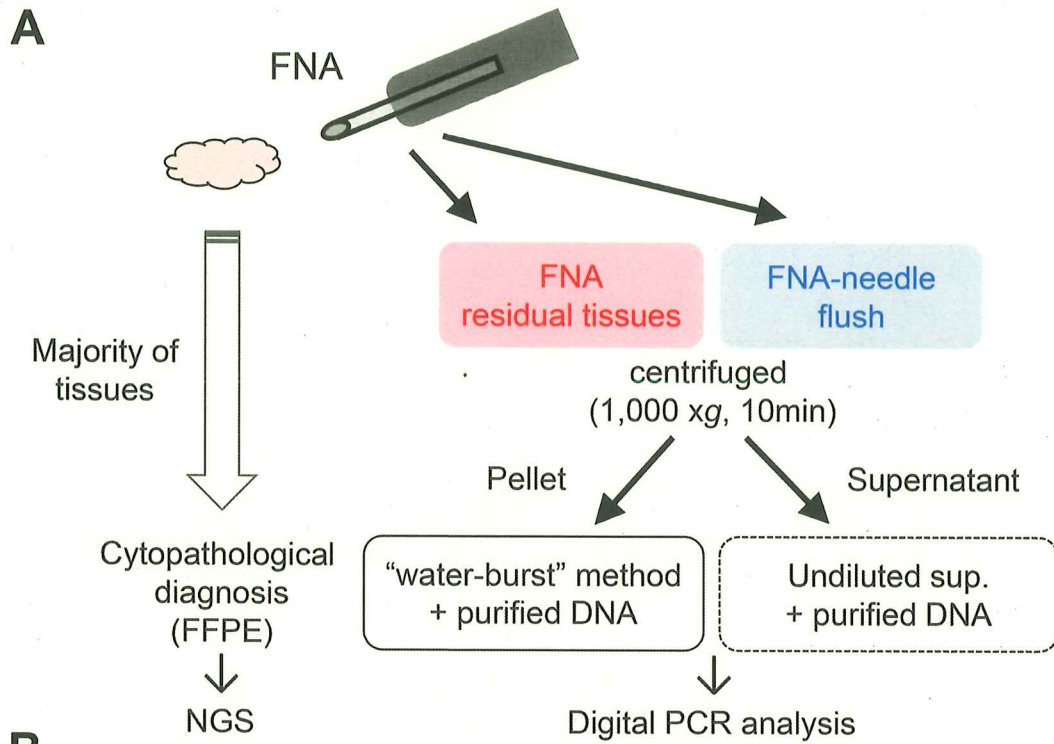
The number of patients included in this study was minimal. Still, to further validate the feasibility for clinical use, it would be necessary to conduct clinical studies with a larger number of patient samples, and test various types of pancreatic tissues using FNA, ranging from benign to malignant tumor tissues. In addition to pancreatic cancer, validation studies are necessary for detecting driver mutations unique to other types of carcinomas, such as the *BRAF* V600E mutation observed during thyroid cancer²⁹, as it would enhance the possibility of developing widespread clinical applications. Specifically, this approach would be clinically relevant for the minimally invasive pathological diagnosis of the tumor with a limited amount of tissue used for sampling. As observed during optional assessments using immunohistochemistry, the direct amplification and detection of key driver mutations would compensate for conventional pathological diagnosis using tissue biopsy and cytopathological analysis. Additional dPCR-based assessment of microsatellite instability may provide more detailed information regarding not only cancer diagnosis but also therapeutic implications.

In conclusion, we developed a digital PCR-based, super-sensitive assay for detecting mutations, which might resolve an issue related to the insufficiency of materials during cytopathological analysis. Our results indicated that a high rate of detection of *KRAS* mutations was associated with small amounts of FNA residual samples. Furthermore, using our “water-burst” method, we showed that even the DNA purification step was not necessary for detecting gene mutations in digital PCR. The straightforward and rapid protocol enables us to perform minimally invasive molecular analysis in cancer clinics.

Methods

Cell lines. Human pancreatic cancer cells (MIA PaCa-2; RCB2094) and non-cancer skin fibroblasts (NB1RGB; RCB0222) were obtained from the RIKEN cell bank (JAPAN), and grown using DMEM (MIA PaCa-2) and α -MEM (NB1RGB) media (FUJIFILM Wako chemicals, Japan) supplemented with 10% fetal bovine serum (GE Healthcare, Chicago, Illinois, USA) and 100 U/mL penicillin–streptomycin (FUJIFILM Wako chemicals). Cell lines were grown at 37 °C with 5% CO₂ and passaged at 70–80% confluence. The number of cells was counted using the Countess automated cell counter (Thermo Fisher Scientific, Waltham, MA, USA).

Patients. To examine the method for detecting mutations using resected tissues, twelve patients with the resectable pancreatic disease admitted in the Sapporo Higashi Tokushukai Hospital between 2017 and 2018 were included. Ten patients from whom FNA residual samples were obtained were recruited from Asahikawa Medical University in 2019. The study protocol for patient tissue collection and scientific analysis was approved by the Tokushukai Group Ethical Committee on Human Research (#TGE00357-012) and Asahikawa Medical University Research Ethics Committee (#17002). The study was conducted in accordance with the Declaration of Helsinki. Written informed consent was obtained from all patients before enrolment.



◀**Figure 2.** *KRAS* mutation analysis using FNA residual tissues via the “water-burst” sample preparation method. (A) Workflow for sample collection and DNA preparation. After submitting patient specimens obtained via FNA for cytopathological diagnosis, residual specimens and the needle washing solution were collected, centrifuged, and separated into a pellet and supernatant. DNA was prepared by the “water-burst” method, in which the precipitate was centrifuged and suspended in water, and dPCR analysis was then performed. The supernatant was directly subjected to the dPCR reaction. These methods do not require DNA purification, and it takes about 2.5 h to obtain genetic information after the collection of a sample. Purified DNA was also subjected to the assay as control (see Table 2). (B) dPCR plot of the *KRAS* G12/G13 mutation assay in the collected tissues were resuspended using water (left large panels). The plot graph shows the pattern of detection of *KRAS* mutations obtained via centrifugation from FNA residual tissues or needle rinsed fluids. The threshold (solid pink line) was manually set to extend to an amplitude of 2,000 or 1,000 (FAM mutant or HEX wild-type probe) above the maximum background intensity value. The asterisk indicates the results for the *KRAS* Q61 mutation assay for patient 9 (right small panels; see Table 2).

Fresh tissue collection and preparation from surgically resected specimens. Small tissue specimens were obtained within 30 min after the surgical resection of the PDA in the operation room. Multiple tumor areas (typically, 2–3 areas) were punctured and aspirated using 22-gauge catheter needles (TERUMO, Tokyo, Japan) connected to 10 mL syringes. The aspirated specimens were suspended in 3 mL of phosphate-buffered saline (PBS) containing 450 μ L of stock solution from the PAXgene Blood ccfDNA Tube (BD Life Sciences; Franklin Lakes, NJ, USA) and stored for up to a week at 4 °C. The suspensions were centrifuged at 1,000 \times g for 10 min at room temperature, and the pellet was resuspended with 12 μ L nuclease-free water, using a 200 μ L pipette tip with a cut tip; this was immediately utilized as a PCR template.

Collection of FNA-residual specimens. After performing FNA-biopsy sampling for cytological diagnosis, FNA residual tissues were obtained using a 22-gauge Franseen biopsy needle (Acquire; Boston Scientific, Marlborough, MA, USA). Residual tissues that remained in the needle were collected in a 5.0 mL microtube by performing aspiration several times (typically, 2–3 times), followed by the emission of 3 mL of physiological saline solution, which was combined with 450 μ L of stock solution from a PAXgene Blood ccfDNA Tube³⁰ by performing inversion and mixing several times and storing the contents for up to a week at 4 °C. Also, we collected needle-wash fluid fractions, to collect the washout tissues. Each suspension was centrifuged at 1,000 \times g for 10 min at 4 °C. The residual pellet fraction was partly scratched and resuspended with 12 μ L nuclease-free water using a 200 μ L pipette tip with a cut tip, and the entire pellet of the needle-wash fraction was resuspended in 12 μ L nuclease-free water. The fraction resuspended in water was directly utilized as a dPCR template. The supernatant fraction obtained after centrifugation was directly input during dPCR. Purified DNA was prepared and used as a control in conventional mutation analysis methods. DNA in the supernatant fraction was purified using a QIAamp MinElute ccfDNA Mini Kit (Qiagen, Hilden, Germany), and the DNA in the pellet fraction was purified with a DNeasy Blood and Tissue Kit (Qiagen).

Mutation detection assay using dPCR. Twenty microliters of the resuspension was mixed with 10 μ L of ddPCR Supermix for Probes (no dUTP; Bio-Rad, Hercules, CA, USA), and 1 μ L of ddPCR *KRAS* Screening Multiplex Kit that targeted *KRAS* exon 2 (#1863506; Bio-Rad) and template DNA solution, and then the mixture was vortexed three times at 2,500 rpm for 1 s. The PCR mixture was mixed with 70 μ L Droplet Generation Oil (Bio-Rad) and compartmentalized using a QX200 droplet generator (Bio-Rad). The kit enables us to screen seven *KRAS* mutations (G12A/C/D/R/S/V and G13D) with a frequency >0.2%, but specific variants cannot be determined. In the case of a tumor harboring *KRAS* Q61 mutation, as determined via NGS, an additional assay was performed using the ddPCR *KRAS* Q61 Screening Kit (Q61K/L/R/H, Bio-Rad), to evaluate the mutation status, with a cut-off >0.5%. Specific variants also cannot be determined.

These mutation detection assays were performed using the following protocol: 10 min at 95 °C, followed by 40 cycles of 30 s at 94 °C, and 60 s at 55 °C, followed by a process for 10 minutes at 98 °C (Ramp Rate; 2 °C/sec, at each step). The threshold for the absolute copy number input during the reaction and the ratio of the mutated fragments was calculated using QuantaSoft (ver 1.7; Bio-Rad), based on the Poisson distribution. Samples were scored as positive for mutant *KRAS* when at least five mutant droplets/reaction were detected using dPCR.

Tumor specimens and mutation analysis. To validate the mutation signature of the tumor, formalin-fixed paraffin-embedded (FFPE) tissue specimens and unstained sections with a thickness of 10 μ m or 4 μ m (resected tissue or FNA biopsy specimen, respectively) were prepared. Genomic DNA was isolated using the GeneRead DNA FFPE Kit (Qiagen), and finally eluted with 30 μ L of elution buffer, as described previously³¹. The purified DNA was quantified using the Qubit dsDNA HS Assay Kit on a Qubit4 fluorometer (Thermo Fisher Scientific).

Somatic mutations in the primary tumor of FFPE tissue specimens were also profiled using targeted amplicon sequencing techniques on the Ion AmpliSeq Custom Next-Generation Sequencing DNA panels, which were designed using the Ion AmpliSeq Designer Website (<https://www.ampliseq.com>), for targeting 8 PDA-related genes, namely *KRAS*, *TP53*, *SMAD4*, *CDKN2A*, *GNAS*, *PIK3CA*, *BRAF*, and *STK11* (Supplementary Table). Details regarding the sequencing analysis are described in the Supplementary Information.

Patient	Age	Sex	FNA (Tumor specimen)			FNA residual tissue				FNA needle flush		
			Pathological diagnosis	Tumor cellularity*	Tumor genotypes (targeted sequencing)	Pellet		Supernatant		Pellet		Supernatant
						Water-burst (%MAF)**	Purified DNA (%MAF)**	Unpurified (%MAF)***	Purified DNA (%MAF)**	Water-burst (%MAF)**	Unpurified (%MAF)***	Purified DNA (%MAF)**
1	74	F	Adenocarcinoma	Mod	KRAS G12V (11.6%)	45.1	17.4	No call	43.4	24.4	No call	39.4
2	50	M	Adenocarcinoma	Low	KRAS G12D (26.9%), TP53 R273H (37.3%)	G12/G13 negative	31.1	No call	32.6	G12/G13 negative	No call	34.9
3	76	F	Adenocarcinoma	Low	KRAS G12R (27.4%), TP53 R273C (33.8%)	44	30	No call	33.8	23.1	No call	14.7
4	59	F	Adenocarcinoma	Mod	KRAS G12D (24.8%), TP53 I195T (32.4%)	20.5	40.9	No call	33.5	24.0	No call	28.6
5	74	M	Adenocarcinoma	Low	KRAS G12D (13.4%), TP53 R273H (20.9%)	11.9	23.9	No call	29.5	21.3	No call	13.3
6	87	F	Adenocarcinoma	Low	KRAS G12C (43.8%), CDKN2A L63Q (24.1%), TP53 H193L (22.9%)	18.9	36.9	No call	34.0	16.0	No call	48.0
7	76	M	Acinar cell carcinoma	High	No mutation call	0.27	G12/G13 negative	No call	G12/G13 negative	G12/G13 negative	No call	G12/G13 negative
8	65	F	Adenocarcinoma	Low	KRAS G12D (10%), TP53 R213X (6%)	19.3	16.0	No call	27.9	G12/G13 negative	No call	19.0
9	43	M	Adenocarcinoma	Low	KRAS Q61R (7.8%)	G12/G13 negative (Q61 mutation; 10.4%)	G12/G13 negative (Q61 mutation; 18%)	No call	G12/G13 negative (Q61 mutation; 8%)	G12/G13 negative (Q61 mutation; 21%)	No call	G12/G13 negative (Q61 mutation; 6%)
10	69	M	Adenocarcinoma	Mod	KRAS G12V (8.2%), TP53 R175H (12.6%)	33.8	42.0	No call	35.5	36.0	No call	37.0

Table 2. Mutation analysis using residual tissues in FNA needles. MAF mutant allele frequency. *Tumor cellularity; High, > 30%; Moderate (Mod), 10–30%; Low, < 10%. **G12/G13 negative; KRAS G12/G13 mutants had a subthreshold prevalence (below 0.2%) relative to the wild-type. ***No call; Neither KRAS mutant nor wild-type allele was detected by digital PCR.

Received: 15 January 2020; Accepted: 23 June 2020

Published online: 23 July 2020

References

- Hewitt, M. J. *et al.* EUS-guided FNA for diagnosis of solid pancreatic neoplasms: a meta-analysis. *Gastrointest. Endosc.* **75**, 319–331 (2012).
- Wang, K. X. *et al.* Assessment of morbidity and mortality associated with EUS-guided FNA: a systematic review. *Gastrointest. Endosc.* **73**, 283–290 (2011).
- Kawabata, H. *et al.* Genetic analysis of postoperative recurrence of pancreatic cancer potentially owing to needle tract seeding during EUS-FNB. *Endosc. Int. Open* **7**, E1768–E1772 (2019).
- Eloubeidi, M. A. *et al.* Yield of endoscopic ultrasound-guided fine-needle aspiration biopsy in patients with suspected pancreatic carcinoma. *Cancer* **99**, 285–292 (2003).
- Da Cunha Santos, G. *et al.* A proposal for cellularity assessment for EGFR mutational analysis with a correlation with DNA yield and evaluation of the number of sections obtained from cell blocks for immunohistochemistry in non-small cell lung carcinoma. *J. Clin. Pathol.* **69**, 607–611 (2016).
- Bor, R. *et al.* Prospective comparison of slow-pull and standard suction techniques of endoscopic ultrasound-guided fine needle aspiration in the diagnosis of solid pancreatic cancer. *BMC Gastroenterol.* **19**, 6 (2019).
- Roy-Chowdhuri, S. *et al.* Concurrent fine needle aspirations and core needle biopsies: a comparative study of substrates for next-generation sequencing in solid organ malignancies. *Mod Pathol* **30**, 499–508 (2017).
- Patra, K. C., Bardeesy, N. & Mizukami, Y. Diversity of precursor lesions for pancreatic cancer: the genetics and biology of intraductal papillary mucinous neoplasm. *Clin. Transl. Gastroenterol.* **8**, e86 (2017).

9. How-Kit, A. *et al.* Ultrasensitive detection and identification of BRAF V600 mutations in fresh frozen, FFPE, and plasma samples of melanoma patients by E-ice-COLD-PCR. *Anal. Bioanal. Chem.* **406**, 5513–5520 (2014).
10. Pupilli, C. *et al.* Circulating BRAFV600E in the diagnosis and follow-up of differentiated papillary thyroid carcinoma. *J. Clin. Endocrinol. Metab.* **98**, 3359–3365 (2013).
11. Luke, J. J. *et al.* Realizing the potential of plasma genotyping in an age of genotype-directed therapies. *J. Natl. Cancer Inst.* **106**, dju214 (2014).
12. Beaver, J. A. *et al.* Detection of cancer DNA in plasma of patients with early-stage breast cancer. *Clin. Cancer Res.* **20**, 2643–2650 (2014).
13. Sho, S. *et al.* Digital PCR improves mutation analysis in pancreas fine needle aspiration biopsy specimens. *PLoS ONE* **12**, e0170897 (2017).
14. Russo, M. *et al.* Tumor heterogeneity and lesion-specific response to targeted therapy in colorectal cancer. *Cancer Discov.* **6**, 147–153 (2016).
15. Vendrell, J. A. *et al.* Detection of known and novel ALK fusion transcripts in lung cancer patients using next-generation sequencing approaches. *Sci. Rep.* **7**, 12510 (2017).
16. Lhermitte, B. *et al.* Adequately defining tumor cell proportion in tissue samples for molecular testing improves interobserver reproducibility of its assessment. *Virchows Arch.* **470**, 21–27 (2016).
17. Dufraing, K. *et al.* External quality assessment identifies training needs to determine the neoplastic cell content for biomarker testing. *J. Mol. Diagn.* **20**, 455–464 (2018).
18. Chen, G., Liu, S., Zhao, Y., Dai, M. & Zhang, T. Diagnostic accuracy of endoscopic ultrasound-guided fine-needle aspiration for pancreatic cancer: a meta-analysis. *Pancreatol.* **13**, 298–304 (2013).
19. Gleeson, F. C., Lee, J. H. & Dewitt, J. M. Tumor seeding associated with selected gastrointestinal endoscopic interventions. *Clin. Gastroenterol. Hepatol.* **16**, 1385–1388 (2018).
20. Kanagal-Shamanna, R. *et al.* Next-generation sequencing-based multi-gene mutation profiling of solid tumors using fine needle aspiration samples: promises and challenges for routine clinical diagnostics. *Mod. Pathol.* **27**, 314–327 (2014).
21. Muller, S. *et al.* Next-generation sequencing reveals novel differentially regulated mRNAs, lncRNAs, miRNAs, sRNAs and a piRNA in pancreatic cancer. *Mol. Cancer* **14**, 94 (2015).
22. Esling, P., Lejzerowicz, F. & Pawlowski, J. Accurate multiplexing and filtering for high-throughput amplicon-sequencing. *Nucleic Acids Res.* **43**, 2513–2524 (2015).
23. Mallampati, S. *et al.* Rational “error elimination” approach to evaluating molecular barcoded next-generation sequencing data identifies low-frequency mutations in hematologic malignancies. *J. Mol. Diagn.* **21**, 471–482 (2019).
24. Ono, Y. *et al.* An improved digital polymerase chain reaction protocol to capture low-copy KRAS mutations in plasma cell-free DNA by resolving “subsampling” issues. *Mol. Oncol.* **11**, 1448–1458 (2017).
25. Huggett, J. F., Cowen, S. & Foy, C. A. Considerations for digital PCR as an accurate molecular diagnostic tool. *Clin. Chem.* **61**, 79–88 (2015).
26. Omori, Y. *et al.* Pathways of progression from intraductal papillary mucinous neoplasm to pancreatic ductal adenocarcinoma based on molecular features. *Gastroenterology* **156**, 647–661 (2019).
27. Alcaide, M. *et al.* A novel multiplex droplet digital pcr assay to identify and quantify kras mutations in clinical specimens. *J. Mol. Diagn.* **21**, 214–227 (2019).
28. Madic, J. *et al.* Three-color crystal digital PCR. *Biomol. Detect. Quantif.* **10**, 34–46 (2016).
29. Fagin, J. A. & Wells, S. A. Jr. Biologic and Clinical Perspectives on Thyroid Cancer. *N. Engl. J. Med.* **375**, 1054–1067 (2016).
30. Schmidt, B. *et al.* Liquid biopsy - performance of the PAXgene(R) blood ccfDNA tubes for the isolation and characterization of cell-free plasma DNA from tumor patients. *Clin. Chim. Acta* **469**, 94–98 (2017).
31. Nagai, K. *et al.* Metachronous intraductal papillary mucinous neoplasms disseminate via the pancreatic duct following resection. *Mod. Pathol.* **33**, 971–980 (2019).

Acknowledgements

We thank Yuko Hayakawa for performing next-generation sequencing analysis of resected tumor and biopsy specimens. We also thank Nobue Tamamura (Asahikawa Medical University) for tissue sample preparation. This study was supported by JSPS KAKENHI via grant number 17K09472, the Suzuken Memorial Foundation, and the Suhara Memorial Foundation; all financial support was provided to Y.M. We would like to thank Editage (www.editage.com) for English language editing.

Author contributions

Y.O., A.H., C.M., and M.S. acquired and analyzed data. Y.O., A.H., and Y.M. designed the study and wrote the article. R.W. and H.K. collected the resected tissues and prepared samples. A.H., H.S., H.K., T.O., and T.G. collected the FNA residual tissues and prepared samples. H.K. and T.O. supervised the study. All the authors critically reviewed the manuscript.

Competing interests

Y.O. and Y.M. received funding from the Hitachi High-Technologies Corporation (Tokyo, Japan). The other authors declare no competing interest.

Additional information

Supplementary information is available for this paper at <https://doi.org/10.1038/s41598-020-69221-6>.

Correspondence and requests for materials should be addressed to Y.M.

Reprints and permissions information is available at www.nature.com/reprints.

Publisher's note Springer Nature remains neutral with regard to jurisdictional claims in published maps and institutional affiliations.



Open Access This article is licensed under a Creative Commons Attribution 4.0 International License, which permits use, sharing, adaptation, distribution and reproduction in any medium or format, as long as you give appropriate credit to the original author(s) and the source, provide a link to the Creative Commons license, and indicate if changes were made. The images or other third party material in this article are included in the article's Creative Commons license, unless indicated otherwise in a credit line to the material. If material is not included in the article's Creative Commons license and your intended use is not permitted by statutory regulation or exceeds the permitted use, you will need to obtain permission directly from the copyright holder. To view a copy of this license, visit <http://creativecommons.org/licenses/by/4.0/>.

© The Author(s) 2020